Journal of Biomechanics 43 (2010) 2999–3006

Contents lists available at ScienceDirect

Journal of Biomechanics

journal homepage: www.elsevier.com/locate/jbiomech
www.JBiomech.com

3D gait assessment in young and elderly subjects using foot-worn inertial sensors

Benoit Mariani [a,*], Constanze Hoskovec [b], Stephane Rochat [b], Christophe Büla [b], Julien Penders [c], Kamiar Aminian [a]

[a] Laboratory of Movement Analysis and Measurements, Ecole Polytechnique Fédérale de Lausanne,-STI-IBI2-LMAM, Station 11/ELH 137, CH-1015 Lausanne, Switzerland
[b] Service of Geriatric Medicine, CHUV & CUTR Sylvana, Epalinges, Switzerland
[c] Holst Centre/IMEC, High Tech Campus 31, Eindhoven, The Netherlands

ARTICLE INFO

Article history:
Accepted 2 July 2010

Keywords:
3D gait analysis
Inertial sensors
Elderly
Foot clearance
Turning

ABSTRACT

This study describes the validation of a new wearable system for assessment of 3D spatial parameters of gait. The new method is based on the detection of temporal parameters, coupled to optimized fusion and de-drifted integration of inertial signals. Composed of two wirelesses inertial modules attached on feet, the system provides stride length, stride velocity, foot clearance, and turning angle parameters at each gait cycle, based on the computation of 3D foot kinematics. Accuracy and precision of the proposed system were compared to an optical motion capture system as reference. Its repeatability across measurements (test-retest reliability) was also evaluated. Measurements were performed in 10 young (mean age 26.1 ± 2.8 years) and 10 elderly volunteers (mean age 71.6 ± 4.6 years) who were asked to perform U-shaped and 8-shaped walking trials, and then a 6-min walking test (6 MWT). A total of 974 gait cycles were used to compare gait parameters with the reference system. Mean accuracy $\pm$ precision was 1.5 ± 6.8 cm for stride length, 1.4 ± 5.6 cm/s for stride velocity, 1.9 ± 2.0 cm for foot clearance, and $1.6 \pm 6.1^\circ$ for turning angle. Difference in gait performance was observed between young and elderly volunteers during the 6 MWT particularly in foot clearance. The proposed method allows to analyze various aspects of gait, including turns, gait initiation and termination, or inter-cycle variability. The system is lightweight, easy to wear and use, and suitable for clinical application requiring objective evaluation of gait outside of the lab environment.

1. Introduction

In clinical setting, gait and mobility are commonly evaluated using questionnaire, observation, or simple functional performance assessments (Tinetti, 1986; Podsiadlo and Richardson, 1991). These evaluations do not require sophisticated equipments and have the advantage of being easy to perform by trained evaluators. However, they are often subjective and dependent on the experience of evaluator. Furthermore, these measures do not allow evaluating specific spatio-temporal gait parameters that have been associated with frequent geriatric syndromes, such as falls, dementia, or frailty (Hausdorff et al., 2001; Kressig et al., 2004; Seematter-Bagnoud et al., 2009). Generally, spatio-temporal gait analysis requires dedicated laboratories with complex systems such as optical motion capture. Recently, ambulatory devices have overcome some of these limitations by using body-worn sensors measuring and analyzing gait kinematics. Unlike standard optical motion capture that requires a dedicated working volume, body-worn sensors can be linked to a light data-logger carried by the subject performing his activities outside the lab with minimal hindrance. Nevertheless, recorded data require appropriate algorithms to compute relevant parameters for clinical use (Aminian, 2006).

Most common gait parameters, such as stride length or gait cycle time, can be obtained from the analysis of foot kinematics. Systems based on Micro-Electro-Mechanical Systems (MEMS) gyroscopes and accelerometers suffer from measurement errors and integration drifts, which limits position and orientation assessment during long-term measurements. However, by placing sensors on foot, drift can be corrected periodically by assuming null velocity of foot during foot-flat period of stance (Curey et al., 2004). Using this hypothesis, Sabatini et al. (2005) proposed a 2D-analysis method with periodic linear drift correction at each stance, and Bamberg et al. (2008) used a similar approach with wireless hardware. However, both studies were restricted to analysis in sagittal plane. Subsequently, Sabatini (2005) used a 3D approach using quaternion for foot orientation and position. Veltink et al. (2003) suggested a method for 3D foot kinematics

* Corresponding author. Tel.: +41 21 693 5627; fax: +41 21 693 6915.
E-mail address: benoit.mariani@epfl.ch (B. Mariani).

0021-9290/$ - see front matter © 2010 Elsevier Ltd. All rights reserved.
doi:10.1016/j.jbiomech.2010.07.003

estimation using ambulatory device for drop-foot stimulator with drift and azimuth resetting at each step. Using additional force sensors, Schepers et al. (2007) applied similar algorithms, focusing on foot placement in forward and lateral directions. Yet, these previous studies were limited to few subjects and the proposed methodologies were not evaluated against any reference instrumentation or only in "optimal" conditions, i.e. during straight walking. Some other studies have been published to track position wearing additional magnetometers (Yun et al., 2007) and/or GPS (Foxlin, 2005), but results remain essentially qualitative and were not validated for use in clinical field.

This study describes a new wearable system based on inertial sensors and dedicated algorithms for precise and accurate assessment of 3D gait spatial parameters. The system is validated in young and elderly subjects during straight walking and turning. The method is based on temporal parameters detection, coupled to an optimized fusion of inertial signals in order to assess 3D gait features outside lab and particularly new parameters such as foot clearance and turning angle.

Fig. 1. S-Sense module with compliant foam attached to shoe.

2. Method

2.1. Foot-worn sensors

A wireless 6-dimensional-inertial measurement unit (6D-IMU) referred as "S-Sense" has been designed (Van de Molengraft et al., 2009). S-Sense module is a small ($57 \times 41 \times 19.5\ mm^3$) and low power (18.5 mA at 3.6 V) stand-alone unit integrating microcontroller, radio transmitter, memory, three-axis accelerometer (ADXL, Analog Device, range 3 g), three-axis gyroscope (ADXRS, Analog Device, roll, yaw with 300 °/s range, pitch with 800 °/s range), and batteries. In this study two S-Sense modules were fixed on shoes at hind-foot position using a compliant foam structure and double-sided Velcro straps (Fig. 1). Raw sensor data were low-pass filtered at 17 Hz, sampled on 12 bits at 200 Hz, and wirelessly transmitted in real time to a PC using "S-Base" receiver plugged in USB. Signals from two S-Senses were synchronized by considering the absolute real time clock sent by the base station to each module at the start of recording. Raw data were preliminary processed to extrapolate some missing data due to wireless data loss or sensor's output saturation (Van de Molengraft et al., 2009). Data from the two feet were finally converted to physical units (g or °/s) using in-field calibration method (Ferraris et al., 1995).

2.2. Reference system

An optical motion capture system (Vicon, Oxford Metrics) with sub-millimeter accuracy was used as reference system (Fig. 2a). Motion capture volume was materialized by a black area of 2.5×5.5 m (Fig. 2b). A dedicated lightweight and rigid structure was designed to attach 3 reflective markers to each S-Sense module (Fig. 2c) in order to measure the 3D position and orientation of the module attached on foot. At each time frame, the 3D position of S-Sense module (P_{ref}) was obtained in fixed frame (XYZ) by arithmetic mean of the position of each marker (M_1, M_2, and M_3). Velocity (V_{ref}) was obtained by simple time derivative of P_{ref}, high frequency noise obtained with this numerical differentiation was further

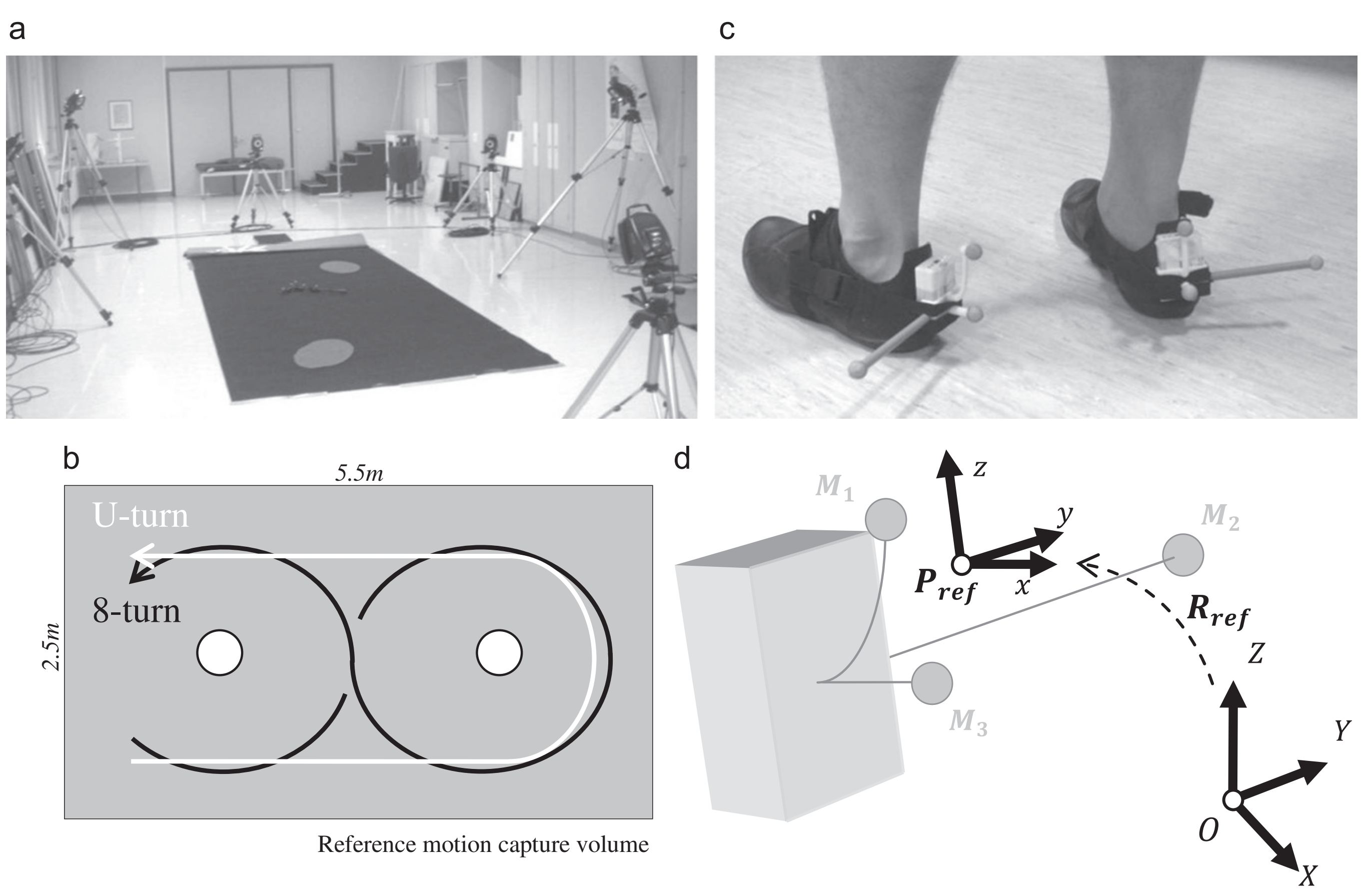

Fig. 2. Experimental Protocol with (a) optical motion capture reference system, (b) gait path during U-turn and 8-turn tasks, (c) markers attached to S-Sense, and (d) reference position (Pref) and orientation (Rref) of the S-sense obtained in fixed frame (XYZ) from markers in mobile frame (*xyz*).

cancelled since only mean velocity over a single gait cycle was considered. Reference 3D orientation of S-Sense mobile frame in XYZ was then expressed as a 3D orientation matrix (R_{ref}) derived from the dimensions of the structure and the vectors defined among markers' positions (Fig. 2d). 3D orientation was also expressed using quaternion representation obtained from matrix representation by classical conversion formulae (Kuipers, 1999).

2.3. 3D foot kinematics estimation

During each gait cycle n, 3D orientation (R_n), velocity (V_n), and trajectory (P_n) of foot were estimated from inertial signals. Practically, this involves the temporal detection of cycles, the knowledge of initial conditions of position and orientation, the gravity cancellation of measured acceleration, and the de-drifted integration of

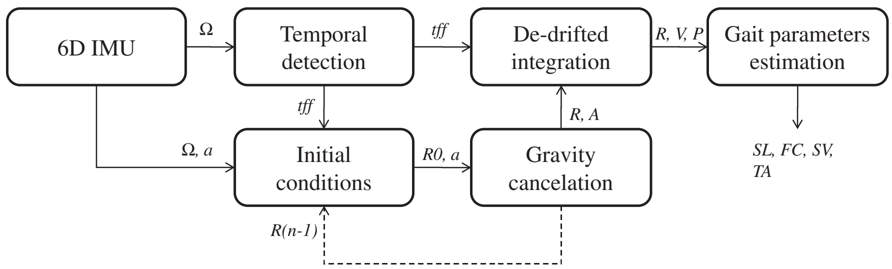

Fig. 3. Block diagram of 3D gait analysis algorithm.

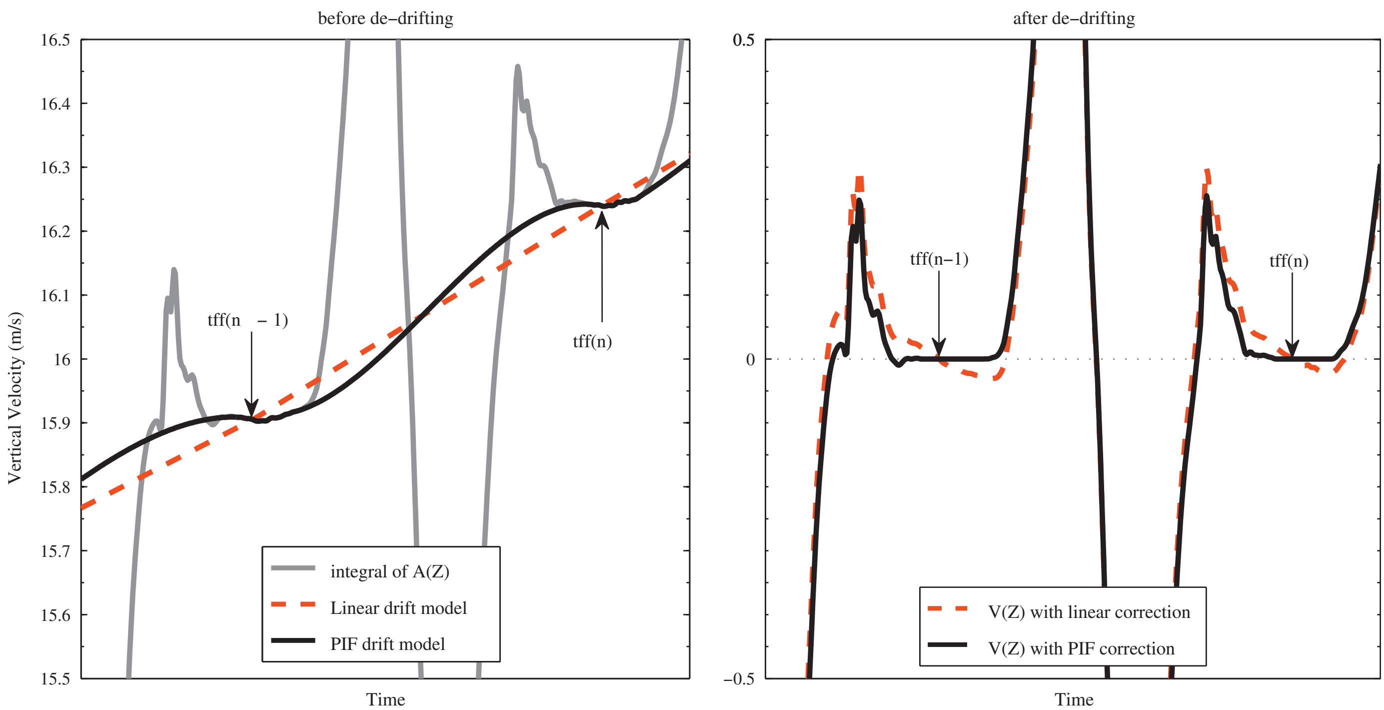

Fig. 4. De-drifted integration of vertical acceleration (A) to obtain vertical velocity (V) using linear function versus p-chip interpolation function (PIF).

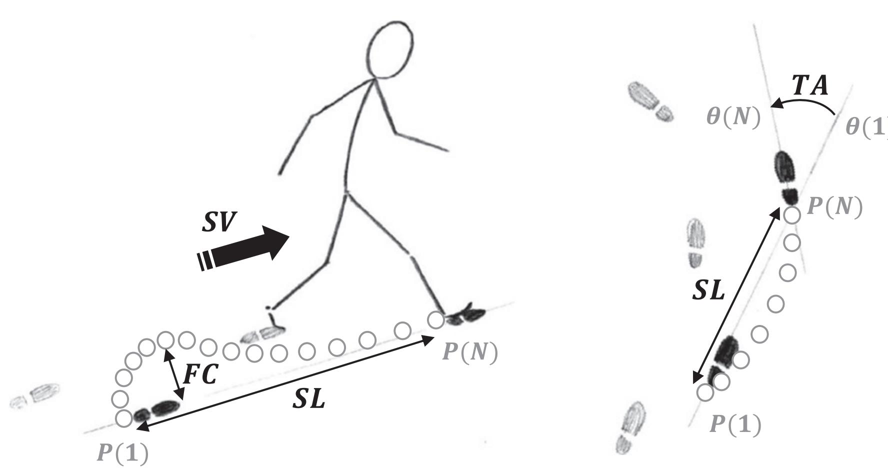

Fig. 5. 3D gait parameters' estimation from 3D foot position (P) and azimuth (θ): stride length (SL), stride velocity (SV), foot clearance (FC), and turning angle (TA).

g-free acceleration. Moreover, kinematics measured by sensors in xyz should be expressed in XYZ to be compared with reference. Fig. 3 illustrates the main algorithmic steps, which are described in the following paragraphs.

Temporal detection of gait cycles was done using angular velocity of foot (Ω) to identify stance phase, adapted from (Salarian et al., 2004). For each stance phase, foot-flat was defined as the continuous period where angular velocity norm was bellowing an empirical threshold. The median of foot-flat period (tff_n) was chosen to separate each gait cycle n.

Initial conditions were updated for each cycle n at tff_n, where the foot was considered motion-less. Initial 3D orientation of S-Sense module ($R0_n$) was obtained by using 3D acceleration (a_n) as inclination (i.e. by aligning z axis with Z), and azimuth was set at the value derived from the orientation at last sample (N) of previous step ($R_{n-1}(N)$).

Gravity cancellation was achieved by aligning the accelerometers' axes (xyz) with fixed frame (XYZ) and subtracting gravity vector. From initial orientation $R0_n$, the orientation of the foot relative to fixed frame ($R_n(i)$) was updated at each time frame ($i=1, 2, \ldots, N$) by a quaternion-based time integration of angular velocity vector Ω_n between two successive foot-flats (tff_{n-1}, tff_n) (Sabatini, 2005; Favre et al., 2008). At each time frame i of cycle n, using measured accelerations ($a_n(i)$), gravity-free component of acceleration in fixed frame ($A_n(i)$) can be summarized by (1).

$$A_n(i) = a_n(i) \times R_n(i) - g, \quad \text{where } g=(0,0,1) \tag{1}$$

De-drifted single and double-integration of gravity-free acceleration (A_n) allowed obtaining 3D velocity and position of foot at each gait cycle n. By assuming that foot velocity is null at each tff_n (Curey et al., 2004), estimation of velocity (V_n) was obtained by trapezoidal integration of A_n. However, this operation involves some drift. Instead of a classic linear de-drifting at each gait cycle, the drift was removed by subtracting a sigmoid-like curve modeled based on a p-chip interpolation function (Carlson and Fritsch, 1985). The p-chip interpolation function (PIF), is defined between the value of $A_{n-1}(tff_{n-1})$ and $A_n(tff_n)$, (Fig. 4). Position (P_n) was finally deduced by simple trapezoidal integration of velocity (V_n).

2.4. Validation protocol and gait parameters

Ten young healthy volunteers (age 26.1 $\pm$ 2.8 years), referred to as "Young" group, and ten fit elderly volunteers (age 71.6 $\pm$ 4.6 years), referred to as "Elderly" group, took part in the study. Among the 20 subjects, there were 9 males and 11 females with height 170 $\pm$ 9 cm. Measurements were scheduled over 2 weeks and protocol was approved by the University of Lausanne ethical committee.

Each subject wearing S-Sense modules on shoes performed three different gait tasks. First, participants walked 5 m straight, turned around a mark, and walked back 5 m (referred as "U-turn"). Second, participants walked around two marks spaced out by 3 m, following a 8 pathway (Tegner et al., 1986) (referred as "8-turn"). Finally, a 6-min Walk Test (referred as "6 MWT") (Crapo et al., 2002) was performed in a 25 m long corridor. U-turn and 8-turn tasks were performed in optical motion capture volume (Fig. 2b). S-Sense was synchronized with reference by maximizing inter-correlation between both the estimated trajectories. Measurements of each task, except 6 MWT, were evaluated a second time after removing completely the system and attaching it again to determine test-retest reliability.

From the 3D foot kinematics, the following four gait parameters were extracted at each cycle n for both reference system and S-Sense using (2), (3), (4) and (5), where N represent the last sample of cycle n:

Stride length (*SL*) was defined as the distance measured between two successive foot-flat positions of the foot. This calculation is valid for curved and turning path as well (Huxham et al., 2006).

$$SL_n = |P_n(N) - P_n(1)| \tag{2}$$

Foot clearance (*FC*) was defined as the maximal foot height during swing phase relative to the height at foot-flat

$$FC_n = \max(P_n(1), P_n(2), \ldots, P_n(N)) - P_n(1) \tag{3}$$

Stride velocity (*SV*) was considered as the mean value of foot velocity in ground plane (XY) during each gait cycle

$$SV_n = \text{mean}\left(V_{n|XY}(1), V_{n|XY}(2), \ldots, V_{n|XY}(N)\right) \tag{4}$$

Turning Angle (*TA*) was defined as the relative change in azimuth (i.e. the projection of orientation in ground plane (*XY*)) between the beginning and the end of gait cycle.

$$TA_n = \theta_n(N) - \theta_n(1) \text{ where } \theta_n = R_{n|XY} \tag{5}$$

Extracted 3D gait parameters are illustrated in Fig. 5.

2.5. Statistical analysis

Instrument comparison—Across each cycle n, we estimated the difference (ε) between optical (reference) and wearable (S-Sense) systems for SL, FC, SV, and TA. Accuracy (mean of ε) and precision (STD of ε) were reported for each of those

Table 1
Correlations and absolute and relative differences between S-Sense and reference system for stride length (SL), foot clearance (FC), stride velocity (SV), and turning angle (TA).

Task	Test	Group	Side	Number of Cyles	ε (SL) R	mean		std		ε (FC) R	mean		std		ε (SV) R	mean		std		ε (TA) R	mean	std
						cm	%	cm	%		cm	%	cm	%		cm/s	%	cm/s	%		deg.	deg.
U-turn				493	95.8	0.9	0.7	6.9	6.4	91.5	2.0	8.1	2.0	8.6	97.0	0.9	0.9	5.7	5.7	99.2	1.6	6.1
8-turn				481	96.2	2.1	1.9	6.6	6.5	91.7	1.7	6.9	1.9	8.1	97.3	2.0	2.1	5.4	5.8	99.4	1.5	6.0
	Test			452	95.8	1.9	1.7	6.7	6.4	92.1	1.8	7.1	2.0	8.2	96.8	1.7	1.9	5.5	5.8	99.1	0.8	6.0
	Retest			522	96.3	1.1	0.9	6.8	6.5	91.1	2.0	7.9	2.0	8.5	97.5	1.2	1.2	5.6	5.7	99.5	2.4	6.1
		Elderly		492	96.0	0.7	0.4	6.1	6.1	92.7	1.2	5.2	1.7	8.1	96.9	0.6	0.7	5.0	5.4	99.5	1.9	4.7
		Young		482	96.0	2.4	2.1	7.5	6.8	90.5	2.6	9.8	2.3	8.6	97.3	2.2	2.4	6.2	6.1	99.1	1.3	7.4
			Right	483	95.2	-0.4	-0.5	6.9	6.8	91.0	1.0	3.7	1.9	7.6	96.9	0.0	0.0	5.7	6.0	99.4	-2.2	6.1
			Left	491	96.8	3.4	3.0	6.6	6.2	92.2	2.8	11.3	2.1	9.1	97.3	2.9	3.0	5.4	5.5	99.2	5.4	6.1
Overall				**974**	**96.0**	**1.5**	**1.3**	**6.8**	**6.5**	**91.6**	**1.9**	**7.5**	**2.0**	**8.4**	**97.1**	**1.4**	**1.5**	**5.6**	**5.8**	**99.3**	**1.6**	**6.1**

estimated gait parameters. Agreement between the two instruments was assessed using graphical way introduced by Bland and Altman (1986). Furthermore, correlation between both systems was calculated, and Student paired t-test was also performed to evaluate the existence of a systematic error.

Repeatability—The test-retest reliability of S-Sense was evaluated by comparing the results of the first and the second trial of each walking tasks. Coefficient of intraclass correlation ICC(1,1) was calculated (Von Eye and Mun, 2006).

Comparisons of groups—Unpaired two-sample t-tests were used to investigate any significant differences between the mean, STD, and CV of gait parameters in elderly and young group during 6 MWT performed with S-Sense.

Significant differences were considered if the null hypothesis can be rejected at the 5% level ($p < 0.05$).

3. Results

3.1. Instrument comparison

Over 1009 gait cycles were obtained with both S-Sense and reference system (corresponding to 20 subjects × 2tasks × 2tests × 2feet × 6–7gait cycles per task), 35 gait cycles (i.e. 3%) were discarded because of reflective markers loss. A total of 974 gait cycles were used consequently for comparison. Table 1 summarizes the differences between the four 3D gait parameters obtained from S-Sense and reference system for the different tasks, tests, groups, and foot sides. Fig. 6 shows the comparison between the parameters obtained from both systems in elderly and young group. Agreement between proposed system and reference was shown in Fig. 7. We found a significant difference ($p < 0.05$) between the two systems, confirming the existence of a small bias (accuracy) in estimating the given gait parameters. We obtained an accuracy ± precision of 1.3 ± 6.5% for SL, 1.5 ± 5.8% for SV, 7.5 ± 8.4% for FC, and 1.6 ± 6.1° for TA. Note that TA estimation error was not evaluated as percentage since its value is sometimes null. Similar differences (ε) were found during U-turn and 8-turn, showing the robustness of the system to turning condition.

3.2. Repeatability

From the mean gait parameters of each subject, (20 “test” and 20 “re-test” samples), ICC(1,1) with 95% confidence intervals were computed for each of the given gait parameters. Results reported in Table 2 show excellent repeatability of mean values (ICC values

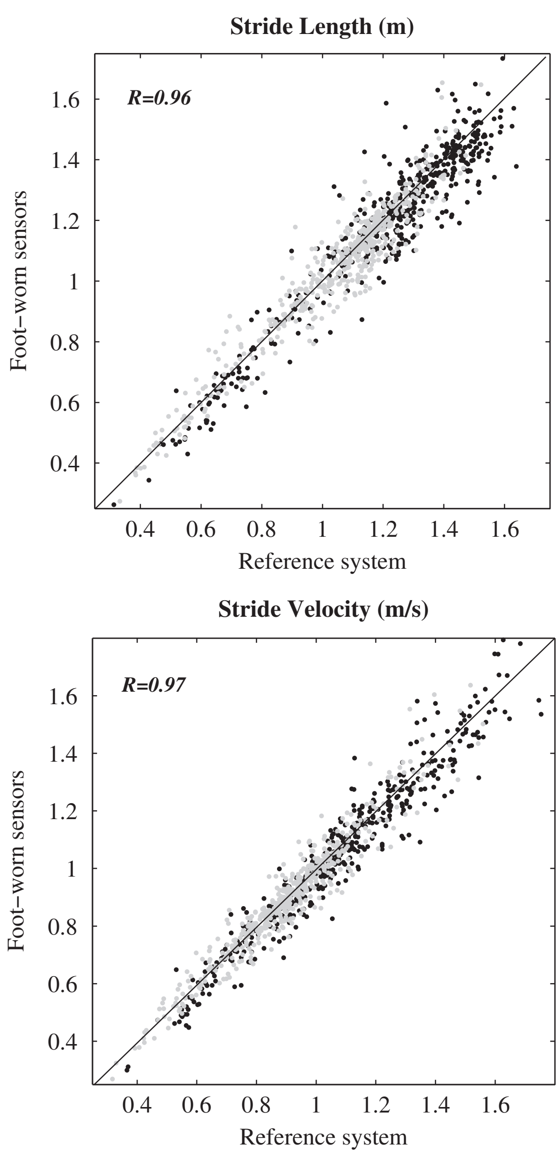

Fig. 6. Comparison of stride length (SL), foot clearance (FC), stride velocity (SV), and turning angle (TA), estimated by foot-worn sensors (S-sense) against reference system for 974 gait cycles in young (●) and elderly (●) subjects.

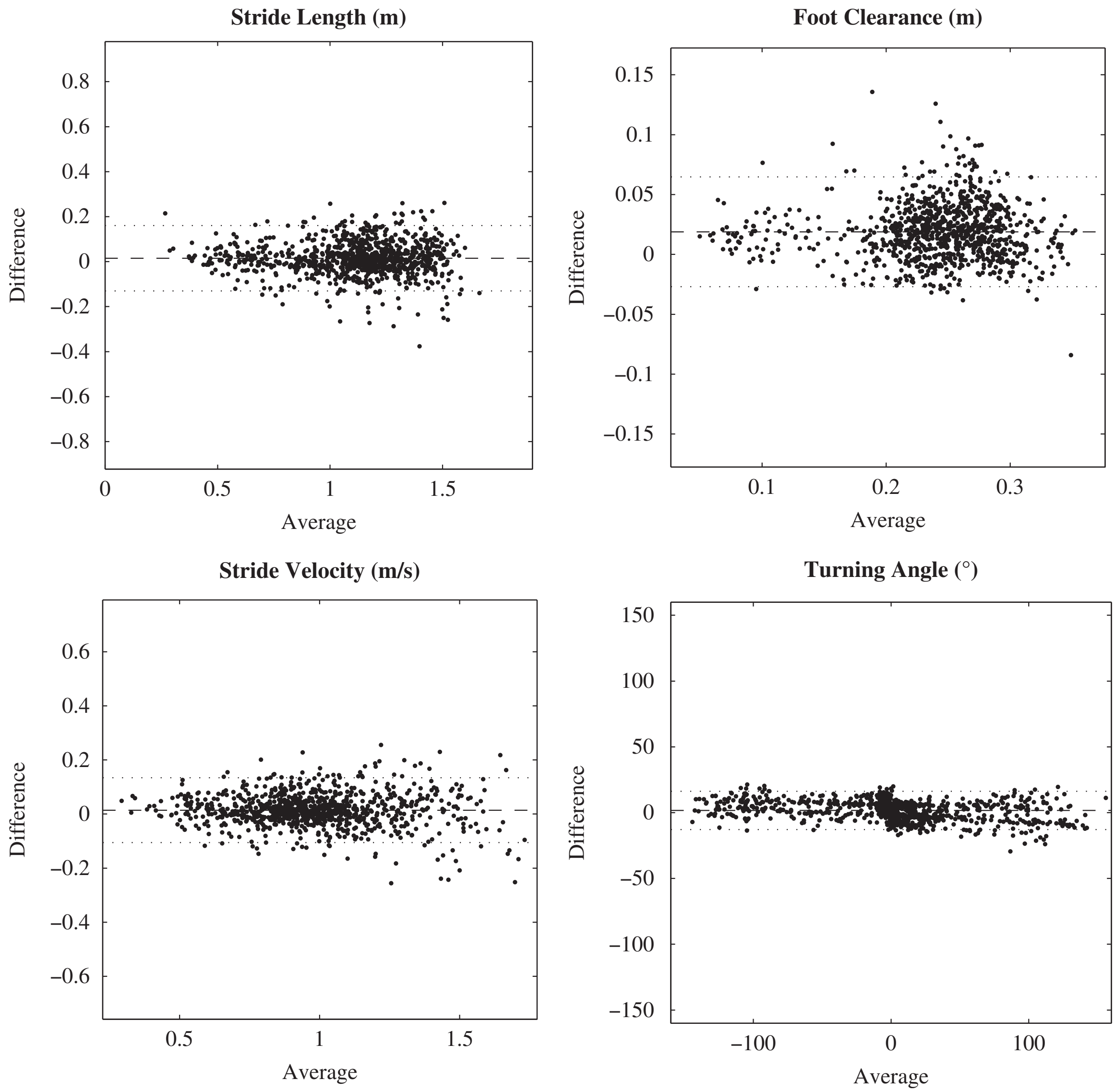

Fig. 7. Bland–Altman plot with mean (*x*-axis) and difference between (*y*-axis) the two values estimated by the wearable system (S-Sense) and reference system across 974 gait cycles in young and elderly subjects. Limits of agreement are specified as average difference (dashed line) ± 1.96 standard deviation of the difference (dotted line).

Table 2
Test-retest reliability of stride length (SL), foot clearance (FC), and stride velocity (SV) during U-turn and 8-turn tasks.

	SL	FC	SV
ICC (1,1)	0.91	0.96	0.93
CI of ICC	[0.79–0.96]	[0.91–0.99]	[0.83–0.97]

above 0.9), according to benchmarks suggested by Menz et al. (2004).

3.3. Comparison of elderly and young subjects

Gait performances of elderly and young subjects were compared during 6 MWT. A total of 10,515 gait cycles were recorded among 20 subjects. Turning angle was used to separate turning periods (every 25 m) and straight walking for analysis. The three other gait parameters were averaged and reported in Fig. 8. Whereas relatively small, non-significant differences ($p > 0.05$), between mean values of SL and SV were observed, FC appeared to significantly discriminate the performance between the two groups ($p=0.02$ for straight walking, $p=0.003$ during turns). Moreover, during turns, SL, SV, and FC were significantly reduced in all subjects compared to period straight walking ($p < 0.015$ for all mean, STD, and CV of those parameters). Interestingly, differences in mean gait parameters between young and elderly groups were larger during turns. We also observed that elderly subjects walked slightly faster than young subjects in straight walking whereas an opposite trend was observed during turning. In addition, mean and STD values obtained during straight walking were consistent with values reported in literature for this population (Winter et al., 1990).

4. Discussion

In this paper we propose a new wearable system with dedicated algorithm for 3D gait assessment and describe validation of its performance against a reference optical motion capture system. A set of original gait parameters is provided that can be

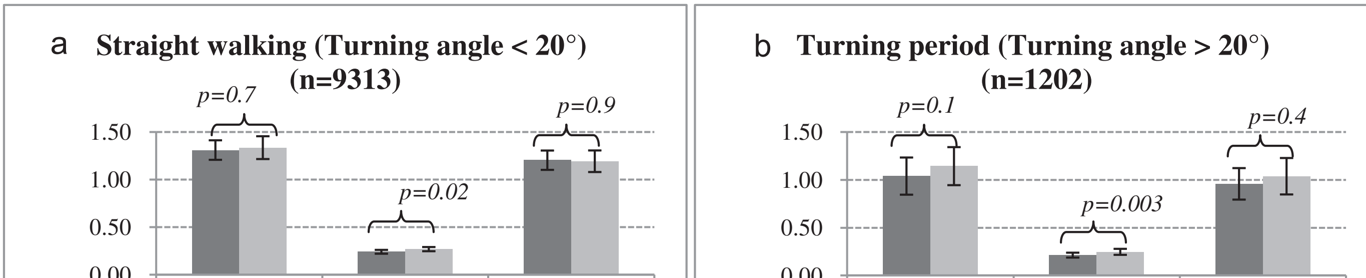

(a)

	SL(m)	FC(m)	SV(m/s)
Elderly	1.31	0.24	1.20
Young	1.34	0.27	1.19

(b)

	SL(m)	FC(m)	SV(m/s)
Elderly	1.04	0.21	0.96
Young	1.14	0.25	1.04

Fig. 8. Comparison of mean stride length (SL), stride velocity (SV), and foot clearance (FC) for elderly and young subjects during 6-min walk test. Significant differences ($p<0.015$) are observed between straight walking (a) and turning (b) for all parameters.

measured when performing normal activity, straight and curved trajectory or during outdoor condition. These parameters show promising preliminary discriminative performance, as they make it possible to distinguish young and elderly subjects.

Hind-foot position of the module was chosen for practical reason, but the proposed algorithm does not require an exact positioning on foot, as illustrated by the high test-retest reliability reported in Table 2. Consecutively, the proposed method could also be applied with sensor worn on other foot positions such as the forefoot. Regarding wireless functionality, frame loss was assessed to 2% during validation protocol, which did not seem to have any influence on the results. However, if consecutive frames were lost, error would become important, so we believe recording of signal on the modules should be better for practical use. We also observed few cases of sensor's saturation with accelerations above 3g at heel-strikes during active walking, especially in the young group. This observation could explain the smaller error observed among elderly subjects (Table 1).

Azimuth (or heading) is tracked from initial position with no correction, thus it is subject to drift. Nevertheless, it has negligible influence on the gait parameters computed at each gait cycle separately, as only overall long-term trajectory is affected. In practice, the proposed system could be used to study 3D foot trajectory during object avoidance, but it would require additional hypothesis or sensors such as magnetometer or GPS for long-term navigation. Even though these sensors might improve the orientation estimation (Luinge, 2002), they are sensitive to nearby mass of iron in the floor for magnetometer, and to satellites occlusion for GPS. Moreover we found that main source of error seems to be mostly in acceleration measure, which may be physically explained by the influence of centrifugal acceleration generated by rotation (Giansanti, 2006).

By considering subjects with various performance and including gait initiation and termination cycles we obtained a wide range of parameters with SL from 30 to 160 cm, turning angle from -150° to 150°, etc…(Fig. 6). This provided a robust evaluation of method's performance in a wide-range of possibilities, and the assessment of various aspects of gait ability such as turning. Compared to other inertial-based gait analysis system (Aminian et al., 2002; Salarian et al., 2004; Sabatini et al., 2005; Schepers et al., 2007), similar or slightly better accuracy and precision was obtained for SL and SV. The method also provides stride-to-stride variability of gait, and previous systems with similar precision were shown to be sensitive enough to identify significant associations between gait variability and various syndromes associated with aging, such as frailty (Seematter-Bagnoud et al., 2009) and fear of falling (Rochat et al., 2010). However, variability estimations, as well as influence of age or gender, should be further investigated in larger population.

The method allows analyzing curved trajectories, it requires fewer sensors' sites and provides new parameters such as TA and FC. Actually, TA is an important outcome to evaluate gait in Parkinson's disease (Zampieri et al., 2010) and FC, which was the most discriminative parameter between our young and elderly subjects, could also be an important new gait parameter to estimate risk of fall in elderly (Begg et al., 2007; Lai et al., 2008). Finally, the system is lightweight and it can be worn directly on user's casual shoes, thus minimizing intrusiveness and interference with normal gait conditions. As a result, volunteers gave a good qualitative feedback on the system, telling they forgot about it while walking. We therefore believe that such a fully wearable device is especially adapted and practical for objective study of gait impairment and daily use in research or rehabilitation centers.

5. Conclusion

The proposed foot-worn system and its outcome parameters were evaluated on a wide range of gait cycles obtained in young and fit elderly subjects, and showed good suitability for clinical gait evaluation. Additional studies are needed to further investigate the applicability of this system when studying frailer elderly subjects with gait impairment. Nevertheless, the current study makes an important contribution to this field of research because this new system provides original gait parameters, such as turning angle and foot clearance, while still maintaining good accuracy and precision for other, commonly used gait parameters (i.e. stride length and stride velocity). The system can be used as an objective tool in many applications requiring gait evaluation in real conditions. It might prove particular relevance to study gait abnormalities during long-term measurements or to investigate the significance of irregularity during turns for outcome evaluation of medical and rehabilitation interventions.

Conflict of interest statement

None.

Acknowledgement

The research leading to these results has received funding from the European Community's Seventh Framework Programme (FP7/2007-2013) under Grant agreement no. 215493.

References

Aminian, K., Najafi, B., Bula, C.J., Leyvraz, P.F., Robert, P., 2002. Spatio-temporal parameters of gait measured by an ambulatory system using miniature gyroscopes. Journal of Biomechanics 35, 689–699.

Aminian, K., 2006. Monitoring human movement with body-fixed sensors and its clinical applications, Invited Chapter in ‘‘Computational Intelligence for Movement Sciences: Neural Networks and Other Emerging Techniques’’. Idea Group Publishers, p. 101–138.

Bamberg, S.J.M., Benbasat, A.Y., Scarborough, D.M., Krebs, D.E., Paradiso, J.A., 2008. Gait analysis using a shoe-integrated wireless sensor system. IEEE Transactions on Information Technology in Biomedicine 12, 413–423.

Begg, R., Best, R., Dell’Oro, L., Taylor, S., 2007. Minimum foot clearance during walking: strategies for the minimisation of trip-related falls. Gait and Posture 25, 191–198.

Bland, J.M., Altman, D.G., 1986. Statistical methods for assessing agreement between two methods of clinical measurement. Lancet 1, 307–310.

Carlson, R.E., Fritsch, F.N., 1985. Monotone piecewise bicubic interpolation. SIAM Journal on Numerical Analysis 22, 386–400.

Crapo, R.O., Casaburi, R., Coates, A.L., Enright, P.L., MacIntyre, N.R., McKay, R.T., Johnson, D., Wanger, J.S., Zeballos, R.J., Bittner, V., Mottram, C., 2002. ATS statement: guidelines for the six-minute walk test. American Journal of Respiratory and Critical Care Medicine 166, 111–117.

Curey, R.K., Ash, M.E., Thielman, L.O., Barker, C.H., 2004. Proposed IEEE inertial systems terminology standard and other inertial sensor standards. In: Proceedings of the Record—IEEE PLANS, Position Location and Navigation Symposium, pp. 83–90.

Favre, J., Jolles, B.M., Aissaoui, R., Aminian, K., 2008. Ambulatory measurement of 3D knee joint angle. Journal of Biomechanics 41, 1029–1035.

Ferraris, F., Grimaldi, U., Parvis, M., 1995. Procedure for effortless in-field calibration of three-axis rate gyros and accelerometers. Sensors and Materials 7, 311–330.

Foxlin, E., 2005. Pedestrian tracking with shoe-mounted inertial sensors. IEEE Computer Graphics and Applications 25, 38–46.

Giansanti, D., 2006. Does centripetal acceleration affect trunk flexion monitoring by means of accelerometers? Physiological Measurement 27 999–1008.

Hausdorff, J.M., Rios, D.A., Edelberg, H.K., 2001. Gait variability and fall risk in community-living older adults: a 1-year prospective study. Archives of Physical Medicine and Rehabilitation 82, 1050–1056.

Huxham, F., Gong, J., Baker, R., Morris, M., Iansek, R., 2006. Defining spatial parameters for non-linear walking. Gait and Posture 23, 159–163.

Kressig, R.W., Gregor, R.J., Oliver, A., Waddell, D., Smith, W., O’Grady, M., Curns, A.T., Kutner, M., Wolf, S.L., 2004. Temporal and spatial features of gait in older adults transitioning to frailty. Gait and Posture 20, 30–35.

Kuipers, J.B., 1999. Quaternions and Rotation Sequences. Princeton University Press.

Lai, D.T.H., Begg, R.K., Taylor, S., Palaniswami, M., 2008. Detection of tripping gait patterns in the elderly using autoregressive features and support vector machines. Journal of Biomechanics 41, 1762–1772.

Luinge, H.J., 2002. Inertial sensing of human movement. Ph.D. Thesis, Twente University Press, Enschede.

Menz, H.B., Latt, M.D., Tiedemann, A., Kwan, M.M.S., Lord, S.R., 2004. Reliability of the GAITRiteÂ® walkway system for the quantification of temporo-spatial parameters of gait in young and older people. Gait and Posture 20, 20–25.

Podsiadlo, D., Richardson, S., 1991. The timed ‘Up and Go’: a test of basic functional mobility for frail elderly persons. Journal of the American Geriatrics Society 39, 142–148.

Rochat, S., Büla, C.J., Martin, E., Seematter-Bagnoud, L., Karmaniola, A., Aminian, K., Piot-Ziegler, C., Santos-Eggimann, B., 2010. What is the relationship between fear of falling and gait in well-functioning older persons aged 65–70 years? Archives of Physical Medicine and Rehabilitation 91 (6) 879–884.

Sabatini, A.M., 2005. Quaternion-based strap-down integration method for applications of inertial sensing to gait analysis. Medical and Biological Engineering and Computing 43, 94–101.

Sabatini, A.M., Martelloni, C., Scapellato, S., Cavallo, F., 2005. Assessment of walking features from foot inertial sensing. IEEE Transactions on Biomedical Engineering 52, 486–494.

Salarian, A., Russmann, H., Vingerhoets, F.J.G., Dehollain, C., Blanc, Y., Burkhard, P.R., Aminian, K., 2004. Gait assessment in Parkinson’s disease: toward an ambulatory system for long-term monitoring. IEEE Transactions on Biomedical Engineering 51, 1434–1443.

Schepers, H.M., Koopman, H.F.J.M., Veltink, P.H., 2007. Ambulatory assessment of ankle and foot dynamics. IEEE Transactions on Biomedical Engineering 54, 895–902.

Seematter-Bagnoud, L., Santos-Eggimann, B., Rochat, S., Martin, E., Karmaniola, A., Aminian, K., Piot-Ziegler, C., Bula, C.J., 2009. Vulnerability in high-functioning persons aged 65–70 years: the importance of the fear factor. Aging Clinical and Experimental Research.

Tegner, Y., Lysholm, J., Lysholm, M., Gillquist, J., 1986. A performance test to monitor rehabilitation and evaluate anterior cruciate ligament injuries. American Journal of Sports Medicine 14, 156–159.

Tinetti, M.E., 1986. Performance-orientated assessment of mobility problems in elderly patients. Journal of the American Geriatrics Society 34, 119–126.

Van de Molengraft, J., Nimmala, S., Mariani, B., Aminian, K., Penders, J., 2009. Wireless 6D inertial measurement platform for ambulatory gait monitoring. In: Proceedings of the 6th International Workshop on Wearable, Micro and Nanosystems for Personalised Health, Oslo, Norway, pp. 63–64.

Veltink, P.H., Slycke, P., Hemssems, J., Buschman, R., Bultstra, G., Hermens, H., 2003. Three dimensional inertial sensing of foot movements for automatic tuning of a two-channel implantable drop-foot stimulator. Medical Engineering and Physics 25, 21–28.

Von Eye, A., Mun, E.Y., 2006. Analyzing rater agreement: manifest variable methods. Applied Psychological Measurement 30, 154–156.

Winter, D.A., Patla, A.E., Frank, J.S., Walt, S.E., 1990. Biomechanical walking pattern changes in the fit and healthy elderly. Physical Therapy 70, 340–347.

Yun, X., Bachmann, E.R., Moore Iv,H., Calusdian, J., 2007. Self-contained position tracking of human movement using small inertial/magnetic sensor modules. In: Proceedings of the IEEE International Conference on Robotics and Automation, pp. 2526–2533.

Zampieri, C., Salarian, A., Carlson-Kuhta, P., Aminian, K., Nutt, J.G., Horak, F.B., 2010. The instrumented timed up and go test: potential outcome measure for disease modifying therapies in Parkinson’s disease. Journal of Neurology, Neurosurgery and Psychiatry 81, 171–176.